Diagn Interv Radiol 2013; 19:387-392

ABDOMINAL IMAGING
ORIGINAL ARTICLE

Clear cell renal cell carcinoma and papillary renal cell carcinoma: differentiation of distinct histological types with multiphase CT

Pal Bata, Janos Gyebnar, David Laszlo Tarnoki, Adam Domonkos Tarnoki, Dora Kekesi, Attila Szendroi, Bence Fejer, A. Marcell Szasz, Peter Nyirady, Kinga Karlinger, Viktor Berczi

PURPOSE
Conventional clear cell renal cell carcinoma (ccRCC) and papillary renal cell carcinoma (pRCC) have different behavioral characteristics and clinical management strategies (nephrectomy vs. nephron-sparing surgery). Our aim was to retrospectively evaluate the contrast enhancement pattern of ccRCC and pRCC and evaluate its possible diagnostic role for preoperative differentiation using a standardized protocol.

MATERIALS AND METHODS
Quadriphasic multidetector computed tomography (CT) images (unenhanced, corticomedullary, nephrographic, and excretory phases) of 19 patients with 20 ccRCC and 14 patients with 15 pRCC lesions (mean ages, 62.3±14.1 and 61.4±13.7 years, respectively) were reviewed retrospectively. The attenuation characteristics were compared with the attenuation of the normal renal cortex using either multiple 10 mm^2 regions of interest or whole tumor attenuation measurements. The degree of contrast enhancement was also compared.

RESULTS
Univariate analysis revealed that ccRCC lesions showed higher mean attenuation values on the corticomedullary and nephrographic phases compared with pRCC masses ($P < 0.05$) using both measurement techniques.

CONCLUSION
The findings underscore the importance of multiphase CT in the differentiation of these two subtypes of RCC using standard assessment techniques. The measurement of the degree of enhancement on contrast-enhanced multidetector CT may be a simple and useful method to radiologically differentiate between the two histological types of RCC.

From the Departments of Radiology (P.B., J.G., D.L.T. ✉ *tarnoki2@gmail.com*, A.D.T., D.K., A.S., B.F., K.K., V.B.), Urology (P.N.) and Pathology (A.M.S.), Semmelweis University School of Medicine, Budapest, Hungary.

Received 20 February 2013; revision requested 24 March 2013; revision received 27 March 2013; accepted 2 April 2013.

Published online 18 July 2013.
DOI 10.5152/dir.2013.13068

The incidence of renal cell carcinoma (RCC) has been rising, with RCC currently accounting for 3% of all adult malignancies (1) and the highest rate occurring in the Central Eastern European region (2). The underlying causes of this increasing incidence of RCC include male gender, aging (50–80 years), obesity, and increasing use of imaging techniques (3–6). The clear cell RCC (ccRCC) histological subtype is characterized by increased neovascularization and relatively frequent vascular invasion and early metastasis (7, 8).

Conversely, another histological type of RCC, papillary RCC (pRCC), is the second most frequent renal malignancy, with an incidence of 10%–15% and a slightly better prognosis compared with ccRCC (9, 10). The 2004 World Health Organization histologic classification of renal tumors defined subtypes of RCC, including pRCC, which bear distinct molecular genetic and histologic characteristics (11). Although most pRCCs are unilateral, they are the most common multifocal or bilateral renal tumors (12).

If pRCC is determined based on computed tomography (CT) appearance preoperatively, nephron-sparing surgery is planned due to the benign behavior of the tumor (less radical surgery is required). Because pRCC is more frequently multicentric and bilateral, residual parenchyma of the contralateral kidney should be considered. Accordingly, radiological differentiation between these two types of renal malignancies would be beneficial.

Due to the development of multiphase CT imaging technology of renal tumors, unenhanced, corticomedullary, nephrographic, and excretory phases can be performed to distinguish the characteristics of various renal malignancies (13). To this end, our aim was to retrospectively analyze the tumor attenuation characteristics in ccRCC and pRCC comparing the attenuation of the normal renal cortex in multiphase CT using a standardized protocol to investigate the possible diagnostic criteria for preoperative differentiation.

Materials and methods

CT scans of 19 patients with either 20 histologically confirmed conventional ccRCC lesions and 14 patients with 15 pRCC lesions who underwent surgical resection were analyzed retrospectively for solid renal lesions at a picture archiving and communication system (PACS Medical workstation, Philips Medical Systems, Shelton, Connecticut, USA) and evaluated by two specialized radiologists who

were unaware of the histological diagnoses. Renal surgeries were performed at the Department of Urology of Semmelweis University, and histology was conducted at the Department of Pathology of Semmelweis University. Institutional review board approval was not required, and no informed consent was obtained from patients because it was a retrospective study.

All multidetector CT scans (Philips Brilliance 16, Philips Healthcare, Amsterdam, The Netherlands) were performed according to a standardized protocol covering the abdomen from the diaphragm to the iliac crest. Nonionic contrast agent (1.5 mL/kg) (Ultravist 370, Bayer AG, Leverkusen, Germany; Optiray 350, Tyco Health/Mallinckrodt, St. Louis, Missouri, USA; or Visipaque 320, GE Healthcare, Waukesha, Wisconsin, USA) was administered, adapted to each weight kg, and was automatically injected at a flow rate of 3 mL/s (14). The patient was placed in the supine position, and each examination phase was performed during expiration.

First, an unenhanced CT scan was performed. Following contrast agent administration, the corticomedullary phase was scanned at 30–45 s, the nephrographic phase at 70–90 s, and the excretory phase at 300–480 s (15). A collimation setting of 16×1.5 mm was used, and the reconstructed slice thickness was 2 mm.

In each patient, three circular regions of interest (ROIs) were drawn in the normal renal cortex (10 mm^2). The most homogeneous and most enhancing (generally peripheral) areas of the solid tumor lesion were measured with the same standard ROI size (excluding necrotic or cystic areas and the normal renal parenchyma). The mean attenuation was calculated in the unenhanced, corticomedullary, nephrographic, and excretory phases and quantified in Hounsfield units (HU). Three measurements were performed in each area in each identical contrast phase at identical points to assess the mean attenuation (Fig. 1). As another measurement, ROIs comprising the complete tumor lesion were again uniformly placed in the slice with the largest diameter of the lesion in each phase (Fig. 2). To reduce possible bias of the measured attenuation due to technical or patient variability, absolute values were normalized using the difference and ratio of attenuation between the tumor lesion and normal renal cortex (16).

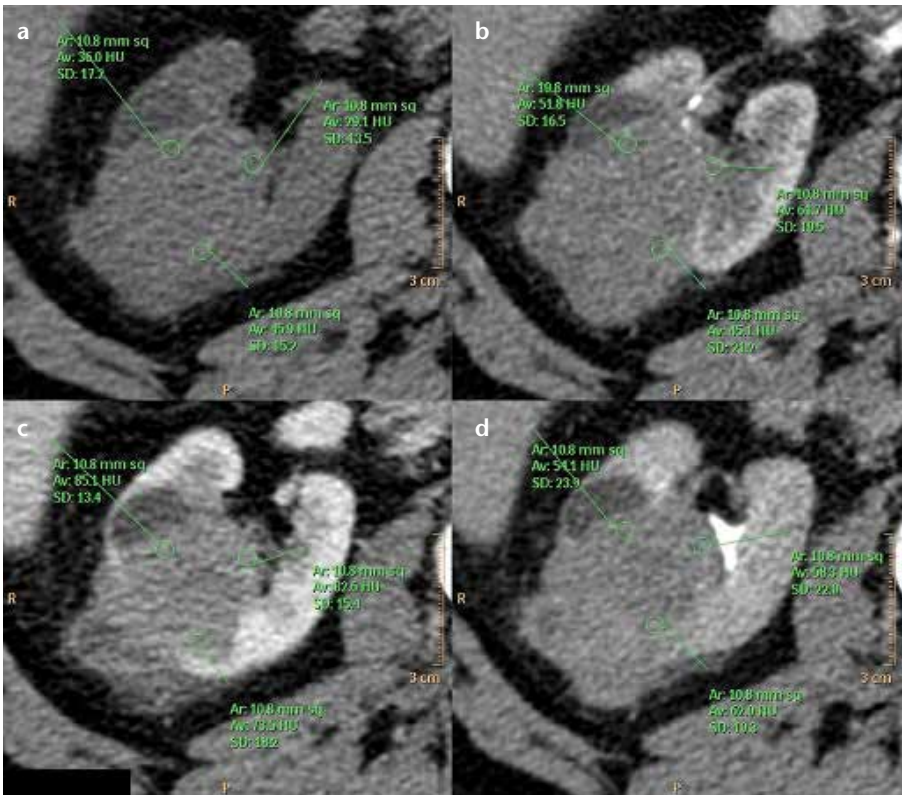

Figure 1. Standardized multidetector CT protocol for measuring mean tumor attenuation with three small 10 mm^2 regions of interest in clear cell renal cell carcinoma. (**a,** unenhanced; **b,** corticomedullary; **c,** nephrographic; **d,** excretory phases).

To evaluate differences in continuous variables, Mann-Whitney U tests were used. *P* values less than 0.05 were deemed to indicate statistical significance.

Results

Nineteen patients with 20 ccRCC lesions and 14 subjects with 15 pRCC lesions were included in the study. Patients presented for CT examination at the CT laboratory between 2009 and 2012. The CT scans were analyzed retrospectively. The mean age of the subjects with ccRCC was 62.3±14.1 years (13 males and six females), whereas the mean age was 61.4±13.7 years for pRCC (11 males and three females). The mean largest diameter of ccRCC was 57.1±37.1 mm and 48.4±39.1 mm for pRCC. When the whole tumor attenuation and small ROI measurement was performed, significant differences were found between the attenuation ratios of ccRCC and pRCC in the corticomedullary (P = 0.009 and P = 0.021, respectively) and nephrographic phases (P = 0.025 and P = 0.012, respectively) (Tables 1 and 2, Figs. 3 and 4). Accordingly, pRCC exhibited greater isodensity to the normal renal parenchyma compared with conventional ccRCC in the above-mentioned investigated phases, and the difference in the attenuation was significant between the two types of tumors using small multiple ROIs (borderline significance in case of nephrographic phase) (Table 1). Using the whole tumor measurement, the difference in the attenuation data of pRCC and ccRCC was insignificant (Table 2).

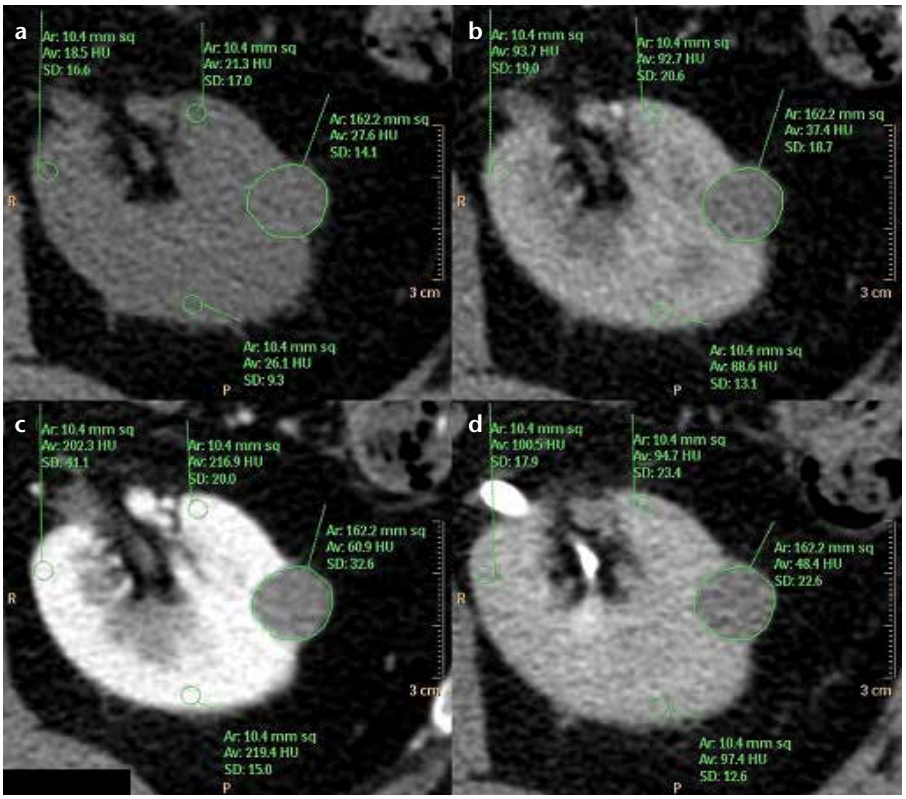

Figure 2. Standardized measurement technique of whole tumor size in each phase for papillary renal cell carcinoma (**a,** unenhanced; **b,** corticomedullary; **c,** nephrographic; **d,** excretory phases).

Table 1. Ratio of and difference in the attenuation between the tumor and normal renal cortex in four-phase CT of clear cell renal cell carcinoma and papillary renal cell carcinoma (ROI size=3×10 mm²)

	Unenhanced	Corticomedullary	Nephrographic	Excretory
Ratio (HU)				
Clear cell RCC (n=20)	1.12 (0.53–1.95)	0.77 (0.25–1.13)	0.72 (0.28–0.92)	0.71 (0.43–1.0)
Papillary RCC (n=15)	1.15 (0.62–2.11)	0.45 (0.23–1.23)	0.43 (0.26–0.95)	0.62 (0.47– 0.76)
P	0.780	0.009	0.025	0.104
Difference (HU)				
Clear cell RCC (n=20)	-3.31 (-15.33–11.87)	34.37 (-22.57–95.2)	42.85 (12.36–130.43)	34.97 (0.3–61.93)
Papillary RCC (n=15)	-3.87 (-25.6–10.33)	60.0 (-10.12–125.33)	72.67 (7.8–161.47)	36.08 (22.52–55.8)
P	0.755	0.028	0.05	0.951

HU, Hounsfield unit; RCC, renal cell carcinoma; ROI, region of interest.
Data are given as median (range).

There was no difference in the attenuation ratio in the unenhanced and excretory phases between the two tumor types.

Discussion

To our knowledge, this is the first study to investigate the contrast enhancement differences of conventional ccRCC and pRCC using two standardized CT diagnostic techniques simultaneously. Significant differences were found in the attenuation ratios between ccRCC and pRCC in the corticomedullary and nephrographic phases using both measurement types (small ROIs vs. whole tumor attenuation)—pRCC generally appeared as a less enhancing lesion compared with the normal renal cortex, and ccRCC appeared more hyperdense than pRCC in these two phases.

Some studies have examined the characterization of renal lesions using morphologic criteria and attenuation measurements (17, 18). Ruppert-Kohlmayr et al. (19) assessed 89 ccRCCs and 16 pRCCs by exclusion of intrinsic factors (e.g., cardiac function, intravenous access, amount of contrast material, weight and size of the patient, blood viscosity) and confirmed—similar to our findings—that there are significant enhancement differences in the corticomedullary and nephrographic phases between the two tumor types if standardized attenuation measurements are used. In the corticomedullary phase, attenuation values of ccRCC were significantly higher (152.6±35.4 HU) than those of pRCC (61.8±24.4 HU; $P < 0.05$). In ccRCC, the mean nephrographic attenuation value was 105.1±17.5 HU. In pRCC, it was 67.3±14.4 HU ($P < 0.05$). However, these differences were diminished by the assessment of relative enhancement (the increase in attenuation after contrast material application) in that study. In the course of the first protocol, the authors compared the attenuation value in the renal lesion with that in the aorta at the level of the supplying vessel (19). We suggest that in this relatively complicated method, the exclusion of intrinsic factors can be omitted by measurement of the attenuation values of the normal renal cortex. Finally, the authors did not use a standard ROI size (they used an ROI that included approximately 1/3 of the lesion) (19). Kim et al. (18) also reported attenuation pattern differences in the same two phases; however, the locations of the ROIs, which varied in size and shape, were decided by consensus of the two radiologists; additionally, the contrast injection parameters and scan delay times varied. To avoid bias in the results, we used a standard, 10 mm² ROI size. We measured the three most homogeneous and con-

Table 2. Ratio of and difference in the attenuation between the tumor and normal renal cortex in four-phase CT of clear cell and papillary renal cell carcinoma (ROIs comprising the complete tumor lesion were placed uniformly in the slice with the largest lesion diameter)

	Unenhanced	Corticomedullary	Nephrographic	Excretory
Ratio (HU)				
Clear cell RCC (n=20)	0.92 (0.58–1.95)	0.54 (0.26–0.98)	0.51 (0.21–0.76)	0.61 (0.35–0.82)
Papillary RCC (n=15)	1.06 (0.66–2.34)	0.38 (0.23–0.71)	0.36 (0.26–0.74)	0.58 (0.40–0.89)
P	0.283	0.021	0.012	0.182
Difference (HU)				
Clear cell RCC (n=20)	2.25	65.43	70.68	43.55
	(-13.30–13.63)	(1.6–115.17)	(30.33–148.60)	(14.5–78.77)
Papillary RCC (n=15)	-1.57	69.67	95.67	38.93
	(-29.00–9.97)	(12.87–153.67)	(37.0–160.13)	(11.33–73.83)
P	0.400	0.330	0.191	0.501

HU, Hounsfield unit; RCC, renal cell carcinoma; ROI, region of interest.
Data are given as median (range).

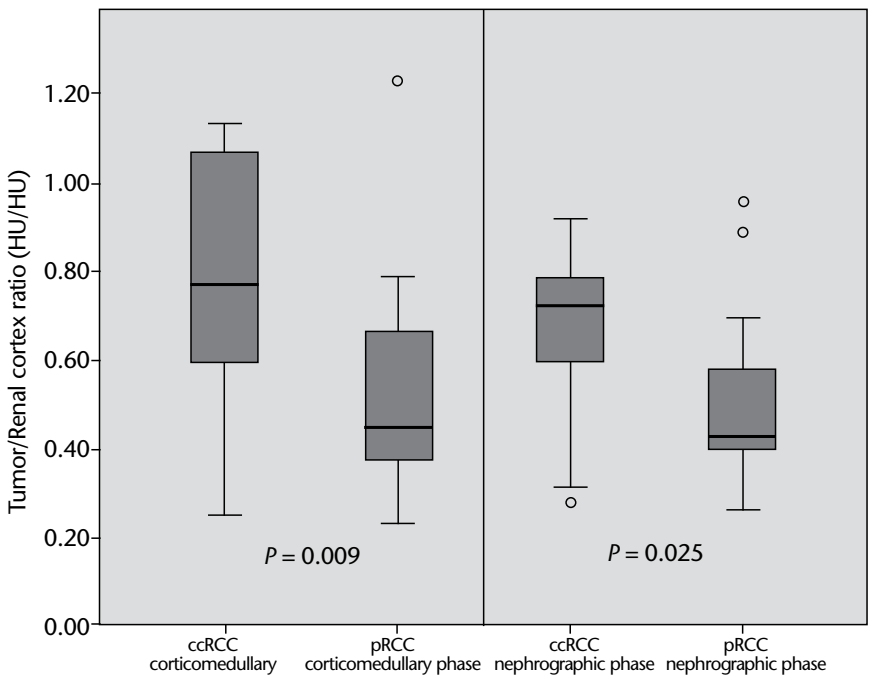

Figure 3. Box and whisker plots of attenuation ratios between the clear cell renal cell carcinoma and papillary renal cell carcinoma tumor lesions in the corticomedullary and nephrographic phases (three small 10 mm^2 regions of interest measured). Boxes represent the range of attenuation from the 25th and 75th percentiles. The horizontal bars indicate the medians, the whiskers represent the 10th and 90th percentile, and circles show the extremes. ccRCC, clear cell renal cell carcinoma; pRCC, papillary renal cell carcinoma.

trast-enhancing small ROIs in the parenchyma or lesion to perform a more precise analysis. For comparison, we also measured the enhancement of the whole tumor. Our findings show that use of a standard ROI size contributes to the significant attenuation differences between ccRCC and pRCC using both techniques.

The significant attenuation differences may be explained by the vascularization characteristics. Conventional ccRCC is known to display improved vascularization, whereas pRCC is typically a hypovascular mass (17, 20). Tumor vascularity can be evaluated *in vivo* using the enhancement parameters of dynamic CT via the heterogeneity of tumor angiogenesis (21). Additionally, Herts et al. (17) reported that although a high tumor-to-parenchyma enhancement ratio (≥25%) excludes the possibility of pRCC, a low tumor-to-aorta enhancement ratio or tumor-to-normal renal parenchyma enhancement ratio is more likely to indicate pRCC. Kim et al. (18) verified that the enhancement pattern is the most useful parameter in differentiating subtypes of RCC. Its heterogeneity between clear cell and nonclear cell types in the corticomedullary phase was defined in a recent study (22).

Additional explanation regarding the pathologic nature of pRCC also helps the understanding of the pattern of its contrast enhancement. pRCC is usually a solid, large well-defined, and slow-growing tumor containing a fibrous capsule (23). Larger pRCC masses show heterogeneity due to necrosis, hemorrhage, calcification, and microscopic fat content. pRCC presents as hypo- or avascular on angiography, a finding that results in minimal enhancement in the cortical phase and hypointensity compared with renal parenchyma in the nephrographic phase. On postcontrast series, pRCC usually enhances homogeneously (23).

Differentiating between the two renal malignancies is essential because of their different therapeutic management strategies and behavior. Because pRCC is related to better prognosis, a minimally invasive strategy (e.g., transcatheter embolization, cryotherapy, or radiofrequency ablation) can be chosen, and total nephrectomy can be avoided (nephron-sparing surgery) (24–26). Additionally, nephron-sparing surgical techniques for pRCC provide an appropriate preoperative staging. Due to the increased likelihood of synchronous or metachronous lesions in papillary RCC, these patients should be followed more closely.

Notably, preoperative fine-needle aspiration biopsy is not part of the

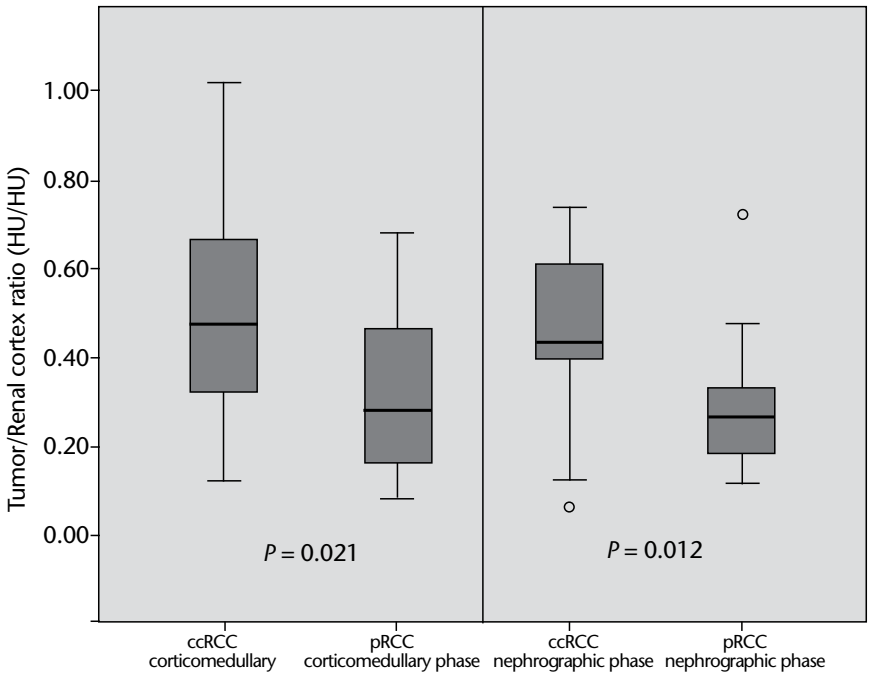

Figure 4. Box and whisker plots of attenuation ratios between the clear cell renal cell carcinoma and papillary renal cell carcinoma tumor lesions in the corticomedullary and nephrographic phases (whole tumor attenuation measured). Boxes represent the range of attenuation from the 25th and 75th percentiles. The horizontal bars indicate the medians, the whiskers represent 10th and 90th percentile, and circles show the extremes. ccRCC, clear cell renal cell carcinoma; pRCC, papillary renal cell carcinoma.

daily routine based on the current guidelines for each patient with renal malignancy; therefore, differentiation using CT characterization is beneficial. Based on our findings, it is important to note that differentiation using the noninvasive attenuation measurement technique can be essential in those patients whose subsequent biopsy cannot be performed due to a higher risk of complications (e.g., bleeding or multiple comorbidities). For a patient with previous unilateral nephrectomy, a second surgery (nephrectomy) could be also avoided. Additionally, systemic treatment choices differ according to the histologic tumor types. A recent study showed that pRCC responds differently to the systemic chemotherapy that has been traditionally used for metastatic ccRCC (27, 28). Furthermore, for metastatic ccRCC, novel biologic agents are available (29).

The present study possesses some limitations. The major limitation is that the number of renal carcinomas, especially that of pRCC, was insufficient for analysis of CT features, although they were comparable to those in previous investigations (16, 18). In fact, this limitation arises from the significantly lower incidence of the pRCC subtype compared with conventional ccRCC. Therefore, further investigation with adequate numbers of these RCC subtypes will be necessary in the future. Second, our analysis was retrospective, and the study population was limited to patients with preoperative multiphase CT examination, a fact that could have biased the selection of both conventional ccRCC and pRCC subjects.

In conclusion, our data suggest a significant difference in the attenuation ratios between conventional ccRCC and pRCC in the corticomedullary and nephrographic phases by multiphase CT using either standard multiple 10 mm^2 ROI sizes or whole tumor attenuation measurement, compared with the density of healthy renal parenchyma. The findings underscore the importance of multiphase CT in the differentiation of these two RCC subtypes using standard assessment techniques.

Conflict of interest disclosure

The authors declared no conflicts of interest.

References

1. Zagoria RJ, Dyer RB, Wolfman NT, Hinn GC, Chen YM. Radiology in the diagnosis and staging of renal cell carcinoma. Crit Rev Diagn Imaging 1990; 31:81–115.
2. Ljungberg B, Steven CC, Han Yong C, et al. The epidemiology of renal cell carcinoma. Eur Urol 2011; 60:615–621. [CrossRef]
3. Taccoen X, Valeri A, Descotes JL, et al. Renal cell carcinoma in adults 40 years old or less: young age is an independent prognostic factor for cancer-specific survival. Eur Urol 2007; 51:980–987. [CrossRef]
4. Verhoest G, Veillard D, Guille F, et al. Relationship between age at diagnosis and clinicopathologic features of renal cell carcinoma. Eur Urol 2007; 51:1298–1304. [CrossRef]
5. Leslie JA, Prihoda T, Thompson IM. Serendipitous renal cell carcinoma in the post-CT era: continued evidence in improved outcomes. Urol Oncol 2003; 21:39–44. [CrossRef]
6. Hu J, Mao Y, White K; Canadian Cancer Registries Epidemiology Research Group. Overweight and obesity in adults and risk of renal cell carcinoma in Canada. Soz Praventivmed 2003; 48:178–185. [CrossRef]
7. Ljungberg B, Hanbury DC, Kuczyk MA, et al. European Association of Urology Guideline Group for renal cell carcinoma. Renal cell carcinoma guideline. Eur Urol 2007; 51:1502–1510. [CrossRef]
8. Kuhn E, De Anda J, Manoni S, Netto G, Rosai J. Renal cell carcinoma associated with prominent angioleiomyoma-like proliferation: report of 5 cases and review of the literature. Am J Surg Pathol 2006; 30:1372–1381. [CrossRef]
9. Mydlo JH, Bard RH. Analysis of papillary renal adenocarcinoma. Urology 1987; 30:529–534. [CrossRef]
10. Storkel S, Thoenes W, Jacobi GH, Lippold R. Prognostic parameters in renal cell carcinoma: a new approach. Eur Urol 1989; 16:416–422.
11. Eble JN, Sauter G, Epstein JI, Sesterhenn IA. WHO classification of tumours: pathology and genetics of tumours of the urinary system and male genital organs. Paris: International Agency for Research on Cancer, 2004.
12. Reuter VE. The pathology of renal epithelial neoplasms. Semin Oncol 2006; 33:534–543. [CrossRef]
13. Cohan RH, Sherman LS, Korobkin M, et al. Renal masses: assessment of corticomedullary-phase and nephrographic-phase CT scans. Radiology 1995; 196:445–451.
14. Birnbaum BA, Jacobs JE, Langlotz CP, Ramchandani P. Assessment of a bolus-tracking technique in helical renal CT to optimize nephrographic phase imaging. Radiology 1999; 211:87–94.

15. Johnson PT, Horton KM, Fishman EK. How not to miss or mischaracterize a renal cell carcinoma: protocols, pears and pitfalls. AJR Am J Roentgenol 2010; 194:307–315. [CrossRef]
16. Gakis G, Kramer U, Schilling D, Kruck S, Stenzl A, Schlemmer HP. Small renal oncocytomas: differentiation with multiphase CT. Eur J Radiol 2011; 80:274–278. [CrossRef]
17. Herts BR, Coll DM, Novick AC, et al. Enhancement characteristics of papillary renal neoplasms revealed on triphasic helical CT of the kidneys. AJR Am J Roentgenol 2002; 178:367–372. [CrossRef]
18. Kim JK, Kim TK, Ahn HJ, Kim CS, Kim K-R, Cho K-S. Differentiation of subtypes of renal cell carcinoma on helical CT scans. AJR Am J Roentgenol 2002; 178:1499–1506. [CrossRef]
19. Ruppert-Kohlmayr AJ, Uggowitzer M, Meissnitzer T, Ruppert G. Differentiation of renal clear cell carcinoma and renal papillary carcinoma using quantitative CT enhancement parameters. AJR Am J Roentgenol 2004; 183:1387–1391. [CrossRef]
20. Zagoria RJ, Wolfman NT, Karstaedt N, et al. CT features of renal cell carcinoma with emphasis on relation to tumor size. Invest Radiol 1990; 25:261–266. [CrossRef]
21. Wang JH, Min PQ, Wang PJ, et al. Dynamic CT evaluation of tumor vascularity in renal cell carcinoma. AJR Am J Roentgenol 2006; 186:1423–1430. [CrossRef]
22. Jung SC, Cho JY, Kim SH. Subtype differentiation of small renal cell carcinomas on three-phase MDCT: usefulness of the measurement of degree and heterogeneity of enhancement. Acta Radiol 2012; 53:112–118. [CrossRef]
23. Gurel S, Narra V, Elsayes KM, Siegel CL, Chen ZE, Brown JJ. Subtypes of renal cell carcinoma: MRI and pathological features. Diagn Interv Radiol 2013 Feb 21. doi: 10.5152/dir.2013.147. [Epub ahead of print] [CrossRef]
24. Dupuy DE. Radiofrequency ablation: an outpatient percutaneous treatment. Med Health R I 1999; 82:213–216.
25. Nadler RB, Kim SC, Rubenstein JN, Yap RL, Campbell SC, User HM. Laparoscopic renal cryosurgery: the Northwestern experience. J Urol 2003; 170:1121–1125. [CrossRef]
26. Roy-Choudhury SH, Cast JE, Cooksey G, Puri S, Breen DJ. Early experience with percutaneous ra- diofrequency ablation of small solid renal masses. AJR Am J Roentgenol 2003; 180:1055–1061. [CrossRef]
27. Choueiri TK, Plantade A, Elson P, et al. Efficacy of sunitinib and sorafenib in metastatic papillary and chromophobe renal cell carcinoma. J Clin Oncol 2008; 26:127–131. [CrossRef]
28. Schrader AJ, Olbert PJ, Hegele A, Varga Z, Hofmann R. Metastatic non-clear cell renal cell carcinoma: current therapeutic options. BJU Int 2008; 101:1343–1345. [CrossRef]
29. Motzer RJ, Basch E. Targeted drugs for metastatic renal cell carcinoma. Lancet 2007; 370:2071–2073. [CrossRef]